

Loss of Function of *Slc20a2* Associated with Familial Idiopathic Basal Ganglia Calcification in Humans Causes Brain Calcifications in Mice

Nina Jensen · Henrik Daa Schröder · Eva Kildall Hejbøl · Ernst-Martin Füchtbauer · João Ricardo Mendes de Oliveira · Lene Pedersen

Received: 12 July 2013 / Accepted: 25 July 2013
© The Author(s) 2013. This article is published with open access at Springerlink.com

Abstract Familial idiopathic basal ganglia calcification (FIBGC) is a neurodegenerative disorder with neuropsychiatric and motor symptoms. Deleterious mutations in *SLC20A2*, encoding the type III sodium-dependent phosphate transporter 2 (PiT2), were recently linked to FIBGC in almost 50 % of the families reported worldwide. Here, we show that knockout of *Slc20a2* in mice causes calcifications in the thalamus, basal ganglia, and cortex, demonstrating that reduced PiT2 expression alone can cause brain calcifications.

Keywords SLC20A2 · Brain calcification · Phosphate transporter · PiT2

Introduction

Familial idiopathic basal ganglia calcification (FIBGC), which formerly was called “Fahr’s disease” and now also is called primary familial brain calcification, is characterized by symmetrical calcifications of the basal ganglia and other brain regions such as the thalamus and cerebellum (Sobrido et al. 2004). The neuropsychiatric and motor symptoms are very heterogeneous, including dementia, psychosis, parkinsonism, dystonia, and migraine. Brain computed tomography has led to more frequent detection of brain calcification, but FIBGC is a rare genetic disease usually with an autosomal dominant inheritance, and there are now clear genetic culprits. Wang et al. (2012) showed that deleterious mutations in *SLC20A2*, encoding the type III sodium-dependent inorganic phosphate (P_i) transporter PiT2, were found in affected families from China, Brazil, and Spain. Thereafter, several other kindred carrying *SLC20A2* mutations were reported in various countries (Schottlaender et al. 2012; Hsu et al. 2013; Lemos et al. 2013; Nicolas et al. 2013; Zhang et al. 2013). The mutation type varies, and some lead to truncated mRNA that is most likely degraded, and some lead to PiT2 proteins that are shown or predicted to be unable to transport P_i (Böttger and Pedersen 2002, 2011; Wang et al. 2012; Hsu et al. 2013; Zhang et al. 2013). Mutations in *SLC20A2* can, however, not account for all cases of FIBGC, and mutations in the *PDGFRB* gene, which encodes a receptor for members of the platelet-derived growth factor family, have also been linked to the disease (Nicolas et al. 2013). It is therefore of great importance to evaluate to which degree the load of PiT2 alone can contribute to the development of brain calcification. To investigate the role of PiT2 in FIBGC, we established *Slc20a2* homozygous knockout mice. We here

N. Jensen · L. Pedersen
Department of Clinical Medicine, Aarhus University,
Aarhus, Denmark

N. Jensen · E.-M. Füchtbauer · L. Pedersen (✉)
Department of Molecular Biology and Genetics, Aarhus University,
C. F. Møllers Allé 3, Building 1130, 8000 Aarhus C, Denmark
e-mail: lp@mb.au.dk

L. Pedersen
Department of Hematology, Aarhus University Hospital,
Aarhus, Denmark

H. D. Schröder · E. K. Hejbøl
Department of Pathology, Odense University Hospital,
Odense, Denmark

J. R. M. de Oliveira
Department of Neuropsychiatry, Keizo Asami Laboratory,
Federal University of Pernambuco, Recife, Brazil

report on 19-week-old *Slc20a2* knockout mice with calcifications in the thalamus, basal ganglia, and brain cortex.

Materials and Methods

Animals

Transgenic C57BL/6N^{Tac} mice (C57BL/6N^{Tac}-*Slc20a2*^{tm1a-(EUCOMM)Wtsi/Ieg} (EM: 05549)) were obtained from the European Mouse Mutant Archive, Germany. The strain is heterozygous for the knockout cassette, L1L2-PGK-P, inserted in *Slc20a2* after exon 2 and flanking exon 3. It introduces splice acceptor and SV40 polyadenylation sequences in *Slc20a2* between the second and third coding exons (<http://www.knockoutmouse.org/martsearch/project/24503>). The mice were housed in the Health Faculty Animal Facility at Aarhus University, Denmark. All mice were fed the same standard diet ad libitum and handled according to the Danish Animal Welfare guidelines. Two 19-week-old mice homozygous for the knockout cassette and two 22-week-old wild-type (wt) mice from the same heterozygous breeding pair (as controls) were sacrificed. The male and female, which were homozygous for the knockout cassette, showed similar patterns of calcifications in their brains, while no calcifications were detected in the male and female wt mice.

Fig. 1 Genotyping and *Slc20a2* mRNA levels. **a** Genotyping of breeders heterozygous for the knockout cassette (-/+) and of homozygous (-/-) and wt (+/+) offspring. *Black arrow*, 500-bp size marker. *White arrows*, 523-bp PCR product derived from wt allele (*upper*) and 443-bp PCR product derived from allele with inserted knockout cassette (*lower*). **b** Tail fibroblasts from a *Slc20a2* knockout mouse (-/-) and three wt mice were lysed, and *Slc20a2* mRNA levels were evaluated by qRT-PCR using primers positioned downstream of the knockout cassette. *Slc20a2* mRNA levels relative to *B2M* are shown. *Error bars* represent standard deviations

Genotyping

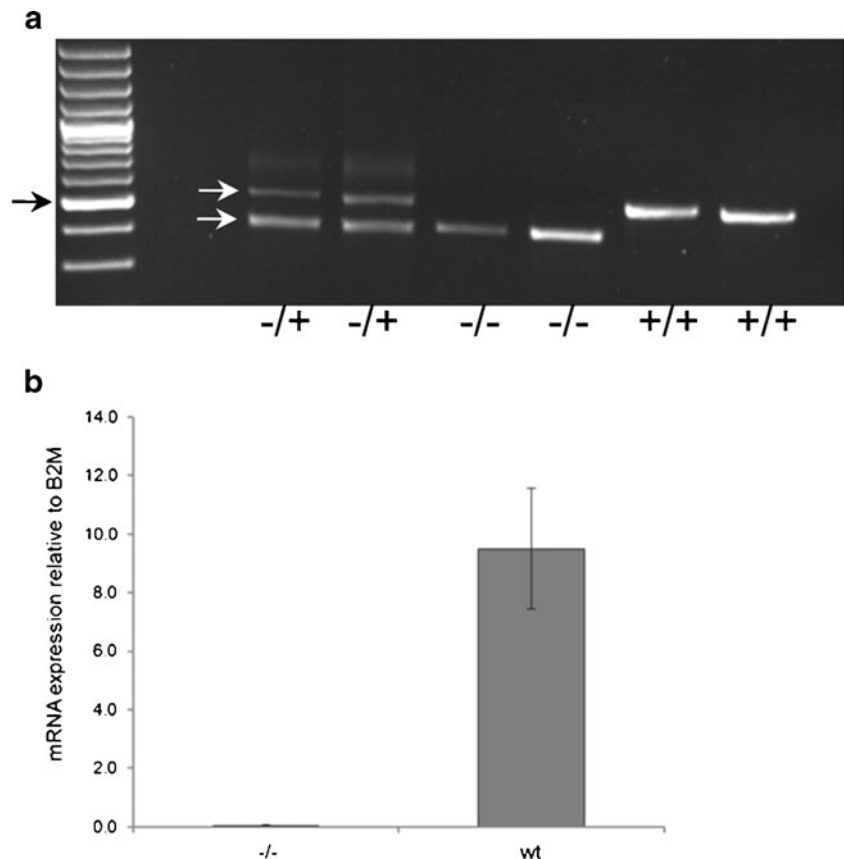
DNA was purified from tail tissue by overnight incubation at 58 °C in Laird's buffer (Laird et al. 1991) (200 mM NaCl, 100 mM Tris-HCl pH 8.5, 5 mM EDTA pH 8.0, 0.2 % SDS) with proteinase K (no. EO0491; Thermo Scientific). The DNA was then precipitated in 2-propanol and redissolved in TE buffer (10 mM Tris-HCl, 1 mM EDTA, pH 8.0). All mice were genotyped by PCR using the Phusion Hot Start II High-Fidelity DNA Polymerase (no. F-549S; Thermo Scientific). Three primers were used: positioned upstream of, downstream of, and inside the L1L2-PGK-P cassette (LAR3), respectively. The sequences of the primers were as follows:

5'arm: 5'-CAGTAGAACTACCGGAAGGAG-3'.
3'arm: 5'-TTGTGCTGCTAGGTGACTGAG-3'.
LAR3: 5'-CAACGGGTTCTTCTGTTAGTCC-3'.

The PCR products were separated by agarose gel electrophoresis using the GeneRuler 100 bp Plus DNA Ladder (Fermentas) as a size marker. The wt and knockout products are 523 and 443 bp, respectively.

Quantitative Reverse Transcription PCR Analysis

Cultured mouse tail fibroblasts were lysed using lysis/binding buffer containing guanidinium thiocyanate provided with the



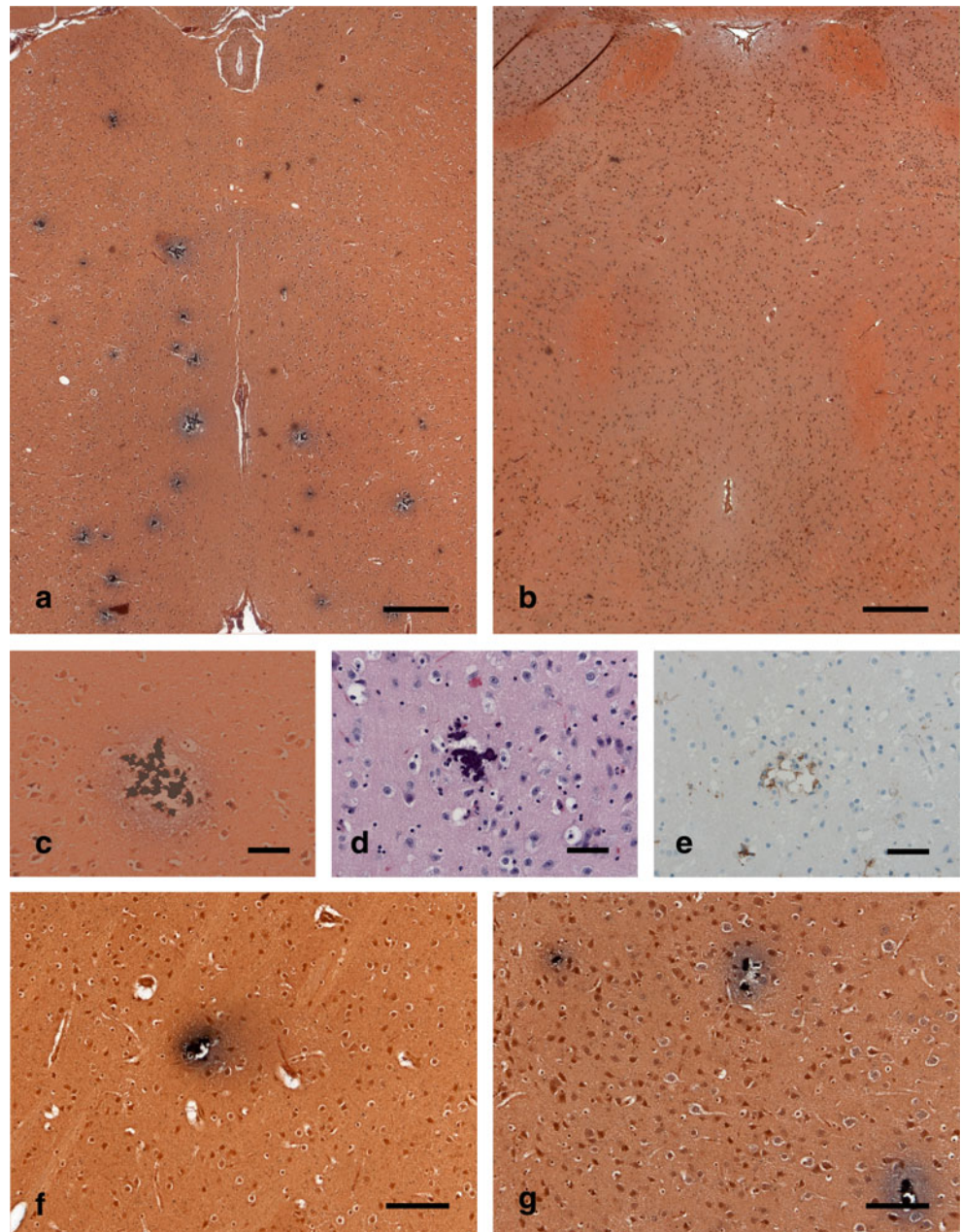
RNAqueous[®]-4PCR Kit (Applied Biosystems). RNA was purified from the lysates using the RNAqueous[®]-4PCR Kit as described by the manufacturer and quantified by UV spectrometry. Immediately after purification, it was reverse transcribed to cDNA using the High Capacity cDNA Reverse Transcription Kit (Applied Biosystems). For quantitative PCR analysis, the following TaqMan[®] Gene Expression Assays (Applied Biosystems) were employed: Mm00660204 (*Slc20a2*) and, as endogenous control, Mm00437762 (*beta-2-microglobulin (B2M)*). The individual quantitative PCR (qPCR) reactions contained 10 μ l TaqMan Fast Universal PCR Master Mix, 1 μ l TaqMan Gene Expression Assay (*Slc20a2* FAM), 1 μ l

TaqMan Gene Expression Assay (*B2M* VIC), and 8 μ l cDNA (approximately 10 ng). The PCR cycles employed were as follows: 95 °C for 10 min and 40 cycles of 95 °C for 1 s and 60 °C for 20 s. The relative mRNA levels were calculated as described in Hellemans et al. (2007). Each qPCR reaction was set up as triplicates.

Histology

Brains were fixed in 4 % paraformaldehyde (formalin 10 % buffered (VWR)) for at least 2 days and then embedded in paraffin. Histological stainings were performed on 4- μ m sections

Fig. 2 Histology of calcifications in brain sections from homozygous *Slc20a2* knockout mouse. **a, b** Von Kossa staining of thalamus regions showing multiple calcifications as black conglomerates in a 19-week-old homozygous *Slc20a2* knockout mouse (**a**), but not in a 21-week-old wt mouse (**b**) (scale bars, 300 μ m). The calcifications are composed of smaller elements seen both in Von Kossa (**c**) and HE (**d**) stainings. In sections stained for macrophages/microglia (F4/80), a tissue reaction is demonstrated (**e**), but not in the wt control (not shown) (scale bars, 50 μ m). Calcifications were also found in other brain regions, as seen by Von Kossa staining of the basal ganglia (**f**) and cortex (**g**) (scale bars, 100 μ m)



from formalin-fixed, paraffin-embedded tissue. The sections were deparaffinized in xylene and rehydrated.

For detection of calcium, sections were stained with the Von Kossa staining technique. The sections were incubated 20 min in 10 % silver nitrate, rinsed in sterile water, followed by 2 min in 5 % pyrogallol. The sections were rinsed again in sterile water and, afterwards, were placed in 5 % sodium thiosulfate for 5 min. For counterstaining, eosin 2.1 % was used.

For immunohistochemical staining, the sections were emerged in H₂O₂ for 10 min to abolish endogenous peroxidase activity. Antigen retrieval was performed by boiling in TEG (10 mM Tris-HCl, 0.5 mM EGTA, pH 9.0) in a microwave oven for 15 min. F4/80 was detected using a rat antibody to murine F4/80 (1:100; AbD Serotec, Bio-Rad). As secondary antibody, a rabbit antibody to rat immunoglobulins (IgG1, IgG2a, and IgG2b) (1:200, E0468; Dako) was used. The sections were then exposed to a goat antibody to rabbit immunoglobulins conjugated with a peroxidase-labeled polymer (Dako EnVision[®]+ System-HRP Labelled Polymer Anti-Rabbit, K4003; Dako). The presence of peroxidase activity was visualized by incubation with DAB+ (K3468; Dako). Lastly, the sections were stained with Mayer's hematoxylin (Ampliqon), to visualize cell nuclei. In between each step, the sections were washed in TNT buffer (Fagron).

Hematoxylin–eosin (HE) staining was performed using a standard protocol. Periodic acid–Schiff (PAS) staining was performed using a standard protocol; Mayer's hematoxylin was used as counterstain.

Results

To establish *Slc20a2* homozygous knockout mice, we used the *Slc20a2*^{tm1a(EUCOMM)Wtsi} allele on a C57BL/6N^{Tac} background obtained from the European Mouse Mutant Archive. The targeting vector introduced a splice acceptor and SV40 polyadenylation sequences between the second and third coding exons in *Slc20a2*, which leads to a premature stop of transcription. The truncated RNA lacks eight downstream coding exons and does not code for any functional gene. Breeding of heterozygous *Slc20a2*^{tm1a(EUCOMM)Wtsi} mice resulted in viable mice homozygous for the mutation (Fig. 1a) in a Mendelian ratio. To test for knockout of *Slc20a2*, we used primers positioned downstream of the knockout cassette and quantified the expression level by a quantitative reverse transcription (RT)-PCR (qRT-PCR) analysis. As seen in Fig. 1b, the mouse homozygous for the knockout cassette shown in Fig. 2 has no expression of *Slc20a2* downstream of the cassette. In sections from the brain, we found extensive, bilateral irregular aggregates of calcified spheres in the thalamus using Von Kossa staining (Fig. 2a). The spheres were about 10 μm in diameter,

and the size of the aggregates was about 50–100 μm (Fig. 2c, d). A few calcifications were also found in the basal ganglia (Fig. 2f) and in the cortex (Fig. 2g). There were no calcifications observed in the cerebellum (not shown). No calcifications were detected in wt controls (Fig. 2b). Tissue reaction to the calcification was demonstrated by immunohistochemistry showing F4/80 positive microglia surrounding the individual elements of the calcified aggregates (Fig. 2e). No other lesions were observed in the brain, and there was no additional focal increase in microglia. The calcifications in FIBGC are believed to initiate in or around blood vessels (Sobrido et al. 2004). Interestingly, PAS staining suggest that this is also the case in the homozygous *Slc20a2* knockout mouse (Fig. 3). The results show that knockout of *Slc20a2* alone is sufficient to cause FIBGC-like calcifications in mice and support the significance of the linkage between mutations in *SLC20A2* and FIBGC.

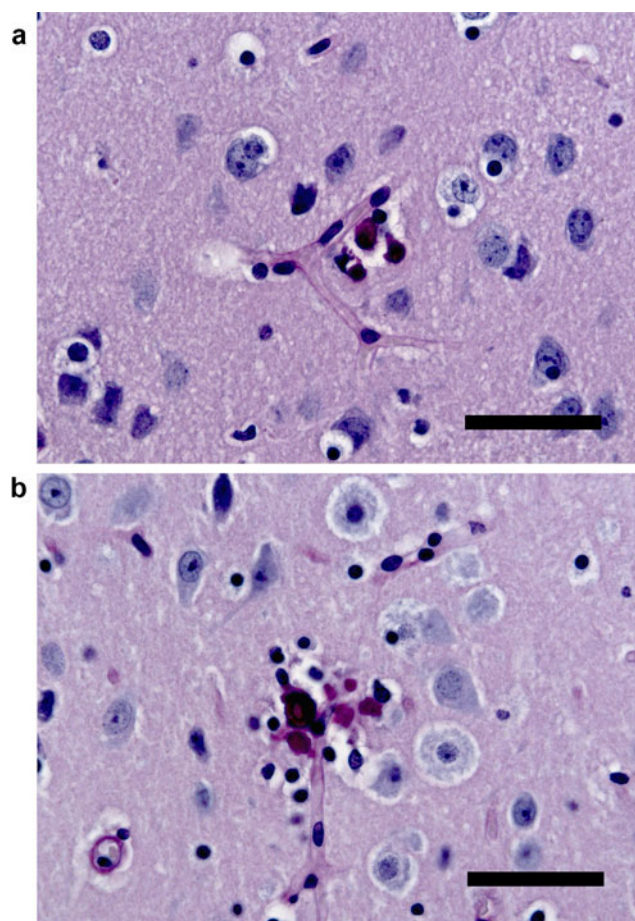


Fig. 3 PAS staining of brain sections from homozygous *Slc20a2* knockout mouse. Calcifications (purple stains) in close relation to blood vessels, delineated by the PAS-positive basal membrane, are found in the basal ganglia (a), thalamus (b), and cortex (not shown) (scale bars, 30 μm). No calcifications/lesions were observed in wt control (not shown)

Discussion

PiT2 has a paralog, PiT1, encoded by the gene *SLC20A1*. The two ubiquitously expressed P_i transporters (Uckert et al. 1998) share some transport characteristics (Böttger et al. 2006), but differ in others (Böttger et al. 2006; Byskov et al. 2012). PiT1 is shown to be involved in calcification in the medial layer of blood vessels (Li et al. 2006; Koleganova et al. 2009), and it is well-accepted that the calcification is a cell-mediated process but debated to which degree vascular smooth muscle cells and pericytes contribute to the calcification. Since the calcifications in FIBGC are believed to initiate in or around blood vessels (Sobrido et al. 2004), and the results on the *Slc20a2* knockout mouse are in agreement with this, it is tempting to speculate that the mechanism is similar to the one involving PiT1, where vascular smooth muscle cells trans-differentiate to mineralizing osteoblast-like cells, possibly caused by elevated extracellular P_i levels (Jono et al. 2000) or by contact with precipitated calcium phosphate products (Sage et al. 2011; Villa-Bellosta et al. 2011). Medial vascular calcification is strongly linked to increased levels of P_i in the blood (Covic et al. 2009). In FIBGC, the blood P_i levels are within the normal range (Sobrido et al. 2004). However, it is possible that a decrease in functional PiT2 leads to a local increase in extracellular P_i. *SLC20A2* and *Slc20a2* have the highest expressions in the affected areas (Lagrué et al. 2010; Silva et al. 2013), and it is, therefore, likely that PiT2 is especially important for maintaining phosphate homeostasis in the affected areas and that only these experience an increase in extracellular P_i concentration. In these areas, the local increase in P_i concentration alone might trigger a cell-mediated mineralization process, or it may lead to passive precipitation of calcium phosphate products, which might trigger a cell-mediated mineralization process, thus leading to an escalation of the calcification. However, the actual mechanism for the development of brain calcifications in the close to 50 % of FIBGC-affected families with an established link to mutations in *SLC20A2* yet remains to be identified. We therefore expect that the *Slc20a2* knockout mouse will develop into an important tool for the study of development of brain calcifications and as a preclinical model for drug testing.

Acknowledgments We thank F. Dagnæs-Hansen and the personnel at the Health Faculty Animal Facility at Aarhus University. The work was in part supported by a grant to LP from the Danish Medical Research Foundation (grant number 09–066064). JRMO was supported by grants from the John Simon Guggenheim Memorial Foundation, CNPq, and FACEPE. NJ was in part sponsored by The Graduate School of Health at Aarhus University.

Conflict of Interest The authors declare no competing financial interests.

Open Access This article is distributed under the terms of the Creative Commons Attribution License which permits any use, distribution, and reproduction in any medium, provided the original author(s) and the source are credited.

References

- Böttger P, Pedersen L (2002) Two highly conserved glutamate residues critical for type III sodium-dependent phosphate transport revealed by uncoupling transport function from retroviral receptor function. *J Biol Chem* 277:42741–47
- Böttger P, Pedersen L (2011) Mapping of the minimal inorganic phosphate transporting unit of human PiT2 suggests a structure universal to PiT-related proteins from all kingdoms of life. *BMC Biochem* 12:21
- Böttger P, Hede SE, Grunnet M, Høyer B, Klaerke DA, Pedersen L (2006) Characterization of transport mechanisms and determinants critical for Na⁺-dependent Pi symport of the PiT-family paralogs, human PiT1 and PiT2. *Am J Physiol Cell Physiol* 291:C1377–87
- Byskov K, Jensen N, Kongsfelt IB, Wielsøe M, Pedersen LE, Haldrup H et al (2012) Regulation of cell proliferation and cell density by the inorganic phosphate transporter PiT1. *Cell Div* 7:7
- Covic A, Kothawala P, Bernal M, Robbins S, Chalian A, Goldsmith D (2009) Systematic review of the evidence underlying the association between mineral metabolism disturbances and risk of all-cause mortality, cardiovascular mortality and cardiovascular events in chronic kidney disease. *Nephrol Dial Transplant* 24:1506–23
- Hellems J, Mortier G, De Paeppe A, Speleman F, Vandesompele J (2007) qBase relative quantification framework and software for management and automated analysis of real-time quantitative PCR data. *Genome Biol* 8:R19
- Hsu SC, Sears RL, Lemos RR, Quintáns B, Huang A, Spiteri E et al (2013) Mutations in SLC20A2 are a major cause of familial idiopathic basal ganglia calcification. *Neurogenetics* 14:11–22
- Jono S, McKee MD, Murry CE, Shioi A, Nishizawa Y, Mori K et al (2000) Phosphate regulation of vascular smooth muscle cell calcification. *Circ Res* 87:E10–17
- Koleganova N, Piecha G, Ritz E, Schirmacher P, Muller A, Meyer HP et al (2009) Arterial calcification in patients with chronic kidney disease. *Nephrol Dial Transplant* 24:2488–96
- Lagrué E, Abe H, Lavanya M, Touhami J, Bodard S, Chalou S et al (2010) Regional characterization of energy metabolism in the brain of normal and MPTP-intoxicated mice using new markers of glucose and phosphate transport. *J Biomed Sci* 17:91
- Laird PW, Zijderfeld A, Linders K, Rudnicki MA, Jaenisch R, Berns A (1991) Simplified mammalian DNA isolation procedure. *Nucleic Acids Res* 19:4293
- Lemos RR, Oliveira MF, Oliveira JRM (2013) Reporting a new mutation at the SLC20A2 gene in familial idiopathic basal ganglia calcification. *Eur J Neurol* 20:e43–44
- Li X, Yang H-Y, Giachelli CM (2006) Role of the sodium-dependent phosphate cotransporter, Pit-1, in vascular smooth muscle cell calcification. *Circ Res* 98:905–12
- Nicolas G, Pottier C, Maltête D, Coutant S, Rovelet-Lecrux A, Legallic S et al (2013) Mutation of the PDGFRB gene as a cause of idiopathic basal ganglia calcification. *Neurology* 80:181–87
- Sage AP, Lu J, Tintut Y, Demer LL (2011) Hyperphosphatemia-induced nanocrystals upregulate the expression of bone morphogenetic protein-2 and osteopontin genes in mouse smooth muscle cells in vitro. *Kidney Int* 79:414–22
- Schottlaender LV, Mencacci N, Koepp M, Hanna M, Hardy J, Lees AJ et al (2012) Interesting clinical features associated

- with mutations in the SLC20A2 gene. *Eur J Neurol* 19(Suppl 1):40
- Silva RJG, Pereira ICL, Oliveira JRM (2013) Analysis of gene expression pattern and neuroanatomical correlates for SLC20A2 (PiT-2) shows a molecular network with potential impact in idiopathic basal ganglia calcification ("Fahr's disease"). *J Mol Neurosci* 50:280–83
- Sobrido MJ, Coppola G, Oliveira J, Hopfer S, Geschwind DH (2004) Primary familial brain calcification. In: Pagon RA et al (eds) *GeneReviews™*. University of Washington, Seattle
- Uckert W, Willimsky G, Pedersen FS, Blankenstein T, Pedersen L (1998) RNA levels of human retrovirus receptors Pit1 and Pit2 do not correlate with infectibility by three retroviral vector pseudotypes. *Hum Gene Ther* 9:2619–27
- Villa-Bellosta R, Millan A, Sorribas V (2011) Role of calcium-phosphate deposition in vascular smooth muscle cell calcification. *Am J Physiol Cell Physiol* 300:C210–C20
- Wang C, Li Y, Shi L, Ren J, Patti M, Wang T et al (2012) Mutations in SLC20A2 link familial idiopathic basal ganglia calcification with phosphate homeostasis. *Nat Genet* 44:254–56
- Zhang Y, Guo X, Wu A (2013) Association between a novel mutation in SLC20A2 and familial idiopathic basal ganglia calcification. *PLoS One* 8:e57060